Polymer Chemistry

Accepted Manuscript

ROYAL SOCIETY OF CHEMISTRY

www.rsc.org/polymers

Journal Name

ARTICLE

Self-Healing Polymers with PEG Oligomer Side Chains Based on Multiple H-Bonding and Adhesion Properties

Received 00th January 20xx,
Accepted 00th January 20xx

DOI: 10.1039/x0xx00000x

www.rsc.org/

Dandan Zhu[†], Qiang Ye[†], Xuemin Lu, Qinghua Lu*

In an attempt to prepare polymers able to function as self-healing materials, quadruple hydrogen-bonding ureidopyrimidinone (UPy) moiety was introduced to polymer systems. Low crosslinking materials based on hydroxyethyl acrylate (HEA) and poly(ethylene glycol) methacrylate (PEGMA) containing 10% of UPy moieties were synthesized, and their thermal and rheological properties were investigated by dynamic mechanical analysis (DMA) and rotational rheometer. The hydroxyethyl group and PEG oligomer with high molecular polarity as side chains provided high surface energies and adhesion property. The fastest self-healing of these polymer films can be finished within 20 min. The adhesion strength tests via tensile mode revealed the potential of these self-healing polymers in application as adhesives.

Introduction

Inspired by natural living organisms where minor damage (e.g., a small cut or bruise) triggers a spontaneous healing response, materials with self-healing or self-repairing capability have attracted considerable interests during the past decades in order to develop artificial materials with improved safety, lifetime, energy efficiency and environmental impact.[1-3] The variety approaches to self-healing materials can be classified into two types: extrinsic self-healing materials and intrinsic self-healing materials. Extrinsic self-healing materials can restore their properties based on the damage-initiated in situ polymerization of healing agents stored in microcapsules,[4-8] particles,[9] or microvascular network[10, 11] embedded in polymer matrix, whereas intrinsic self-healing materials are relying on reversible bonds, including non-covalent[12-17] or dynamic covalent bonds.[18-21] For most of intrinsic self-healing materials, external stimuli are required to achieve healing. For example, a metallo-superamolecular polymer was reported by Rowan et al. to be optically healable by converting photonic energy into heat.[22] Sun and coworkers recently reported a layer-by-layer film based on polyelectrolyte film (polyethyleneimine, PEI) with good self-healing performance with the assistance of water.[23] Also, some gel systems have been reported to be able to self-heal at room temperature, but the healing process requires a large amount of solvent.[24-26]

Recently, some examples of materials have shown the ability to spontaneously self-heal at ambient temperature based on hydrogen bond.[17, 27, 28] Guan and coworkers developed an autonomic self-healing thermoplastic elastomers based on hydrogen bond by combining enhanced stiffness and toughness with the dynamic supramolecular assemblies.[29] Hence, hydrogen bond has been proved a promising candidate for fabrication of bulk polymers with repeatable healing process that requires no external energy. Hydrogen-bonded dimers of ureidopyrimidinone (UPy), of which the dimerization strength ($\Delta G°_{dim}$ = -35 kJ/mol in chloroform) is intermediate between the bond strength of covalent and of most other noncovalent bonds, have been used and acted as robust, selective and directional hydrogen-bonding systems in various supramolecular polymers and reversible networks since the first report by Meijer.[30] Recently, a few self-healing polymers based on quadruple H-bonding UPy group were reported.[31] Interestingly, Zeng and coworkers fabricated a self-healing PBA-UPy polymer and studied its surface interactions and adhesion mechanism.[32]

Poly(ethylene glycol) (PEG), containing repeating polar ether bonds in main chain, compared with most of acrylic polymers like poly(butyl acrylate) (PBA) and poly(ethyl acrylate) (PEA), presents higher molecular polarity and consequent higher surface energy which means of providing better adhesion capability. What is more, PEG shows excellent biocompatibility, leading to its wide investigation as biocompatible materials like hydrogels.[33-35] It has been reported that the length of PEG oligomer as side chain is correlated to material properties.[36, 37] Therefore, it will be fascinating to construct PEG-based adhesives with self-healing ability, which maybe not only self-heal the cracks between different substrate surfaces via regulating the T_g and mechanical properties by molecular design, but also present possibility to be used in tissue engineering, such as to adhere wounded skin tissue of organisms and promote wound healing. However, to now, there is still no report about employing PEG to achieve this kind of adhesives.

School of Chemistry and Chemical Engineering, State Key Laboratory of Metal Matrix Composites, Shanghai Jiao Tong University, Shanghai 200240, China. e-mail: qhlu@sjtu.edu.cn
[†]These authors contributed equally to this work.
Electronic Supplementary Information (ESI) available: NMR, FTIR, DMA, Rheological studies. See DOI: 10.1039/x0xx00000x

In this work, we reported the preparation of self-healing polymers using hydroxyethyl group and PEG oligomers with different length as side chains based on multiple H-bonding of UPy. The effects of side chains on material properties were investigated by rheological investigation. The films of these copolymers can spontaneously self-heal the cracks under ambient environments. These copolymers presented high surface energies, and the adhesion strength tests indicate the copolymers had potential as adhesives with self-healing abilities and possibility to work in different temperatures. Furthermore, the capability of self-healing the crack interfaces of the copolymers with PEG oligomers as side chains may provide them potential applications in tissue engineering as wound-healing promoter. This might be the first attempt in self-healing polymers based on PEG with adhesion property.

Experimental

Materials

2-Isocyanatoethyl methacrylate, 6-methylisocytosine, and N, N'-methylenediacrylamide were purchased from J&K Scientific Co. and used as received. Monomers 2-hydroxyethyl acrylate (HEA) and poly(ethylene glycol) methacrylate (Mn = 360 and 500, $PEG_{360}MA$, $PEG_{500}MA$) were purchased from Aldrich and passed through a neutral alumina column to remove inhibitor before use. Initiator azodiisobutyronitrile (AIBN) was purchased from J&K Scientific Co. and used after recrystallization in ethanol. Solvents were purchased from National Pharmaceutical Group Chemical Reagent Co. Dimethyl sulfoxide (DMSO) was dried over CaH_2 and distilled under reduced pressure. All other reagents and solvents were used as obtained unless otherwise specified.

Preparation of polymers

The UPy-functionalized monomer 2-(3-(6-methyl-4-oxo-1,4-dihydropyrimidin-2-yl)ureido)ethyl acrylate (MAUPy) was synthesized as reported previously.[38] The monomers 2-hydroxyethyl acrylate (HEA), $PEG_{360}MA$ and $PEG_{500}MA$, which have different length of $-CH_2CH_2O-$ group, were selected. The copolymerization of MAUPy with HEA, $PEG_{360}MA$ or $PEG_{500}MA$ was perfomed using the trithiocarbonate 2-(((dodecylthio)carbonothioyl)thio)-2-methylpropanoic acid ($C_{12}TTC$) as the RAFT chain transfer agent for reversible addition-fragmentation chain transfer polymerizaion,[39] 2,2-azobisisobutyronitrile (AIBN) as the radical initiator, and N, N'-methylenediacrylamide as cross linker. The obtained copolymers were named PHEA-UPy, $PPEG_{360}$-UPy and $PPEG_{500}$-UPy, respectively. A control polymer $PPEG_{500}$ was also synthesized from $PEG_{500}MA$ and cross liker in the absence of MAUPy.

Preparation of samples for tensile test

The 180° peer test was carried out under tensile mode to investigate the adhesion strength of the copolymers. The samples were prepared as follows: the melted copolymers were deposited onto the smaller surfaces of two L-shaped steel substrates with a coating thickness of about 0.2 mm. Then the surfaces with coated polymers were overlapped, the jointed substrates were treated at temperature above T_g for 30 min. Then the adhesion strength measurements were carried out via tensile mode at ambient environment.

Measurements

The NMR spectra were obtained from a MERCURY plus 400 (Varian, Inc., USA) Nuclear Magnetic Resonance spectrometer using tetramethylsilane (TMS; δ=0) as internal reference. The FTIR analysis was performed on a Spectrum 100 FT-IR spectrometer (Perkin Elmer, Inc., USA). Mechanical properties were tested on a DMA 7e dynamic mechanical analyzer (Perkin Elmer, Inc., USA). The rheological measurements were carried out using a MCR302 rotational rheometer (Anton paar, Austria) with parallel-plate geometry (diameter of 25 mm). The microscopic photos were taken on an inverted fluorescence microscope (IX 71, Olympus) equipped with a charge-coupled device (CCD) camera. The contact angle tests with three probe liquids (water, diiodomethane and ethyleneglycol) were carried out on a Contact Angle System OCA20 (DataPhysics Instrument GmbH, Germany) in air at room temperature. The tensile experiments were performed on an Instron 4465 universal test machine (Instron Corp., USA).

Results and discussion

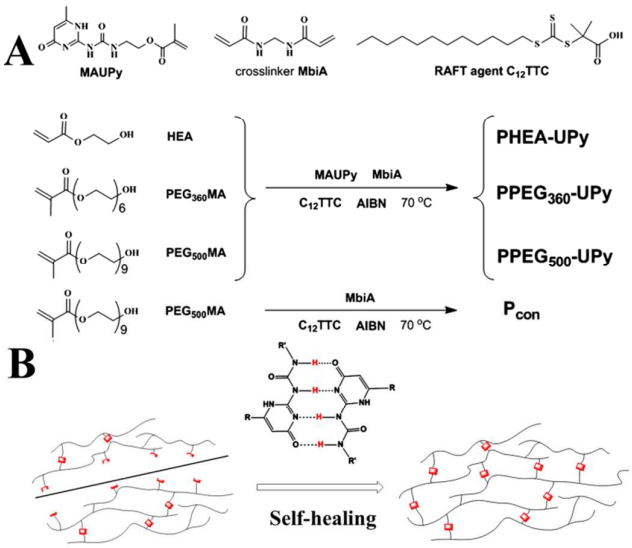

Scheme 1. Chemical structure of the reagents and preparation of polymer PHEA-UPy, $PPEG_{360}$-Upy，$PPEG_{500}$-UPy and control polymer $PPEG_{500}$ (A), and illustration of the self-healing based on quadruple hydrogen bonding interaction of UPy dimers (B).

Synthesis

The chemical structure of monomers and the polymerization reaction were shown in Scheme 1a. The NMR spectra of MAUPy monomer and $C_{12}TTC$ were shown in

1-4, indicating the successful synthesis. The employment of HEA and poly(ethylene glycol) methacrylate was expected to regulate the copolymer properties by different length of side chains with high polarity. The copolymers were prepared with same molar ratio (monomer/MAUPy/cross linker = 86/10/4) for each system.

The characterization of the polymers

^{1}H NMR and FTIR were employed to characterize the structures of polymers. The peaks of protons in UPy groups were clearly observed in Figure S7. As shown in the FTIR spectra in Figure S6, the characteristic vibration peak of C = C (UPy) can be clearly found at 1587 cm^{-1}, and the characteristic vibration peak of C = O (UPy) appeared at 1661 cm^{-1} for the prepared polymers. These peaks are consistent with those characteristic vibration peaks of UPy moiety in FTIR spectrum of monomer MAUPy. And for FTIR spectrum of the polymer $PPEG_{500}$, no peak was observed at 1587 cm^{-1}. This result demonstrated the presence of H-bonding moiety UPy in polymers PHEA-UPy, $PPEG_{360}$-UPy and $PPEG_{500}$-UPy.

Table 1. Summary of T_g values of the prepared copolymers.

Polymer	PHEA-UPy	$PPEG_{360}$-UPy	$PPEG_{500}$-UPy
Feeding molar ratio[a]	86/10/4	86/10/4	86/10/4
T_g (DMA, °C)	45	-22	-33

[a] The feeding molar ratio of HEA($PPEG_{360}$ or $PPEG_{500}$-UPy)/MAUPy/cross linker.

The glass transition temperature (T_g) of the polymers were measured by dynamic mechanical analysis (DMA) in tensile mode (heating rate 3 °C/min, frequency 1 Hz). The maximum in the loss tangent (tan δ) was taken as the T_g value. A steel sample holder was employed in the DMA experiment. Table 1 summarizes the T_g of the three copolymers. It can be clearly observed that the PHEA-UPy polymer has the highest T_g of 45 °C due to its short side chain length of HEA and extending the length of side chains leads to the decrease of T_g. It is notable that the copolymer PHEA-UPy exhibited a T_g which is almost 30 °C higher than that of homopolymer PHEA (T_g, ~15 °C).[40] And the control polymer presented an even lower T_g value (~-53°C) than $PPEG_{500}$-UPy due to the absence of the UPy moiety. According to previously reported,[32] 7.2% UPy in the poly(butyl acrylate)-UPy copolymers led to a 22°C higher T_g. Therefore, the enhanced T_g of the UPy-based copolymers is owing to the enhanced intermolecular interactions by the multiple hydrogen-bond group UPy. The TGA measurements showed in Figure S8 demonstrated the three prepared polymers didn't thermally decompose at temperature below 200 °C.

Bulk rheological analysis

Rheological characterization can provide insight into the properties of bulk polymers. The rheological properties of the UPy-based polymers were evaluated by using a parallel plate rheometer at 25 °C. Strain amplitude sweep was carried out to analyze the elastic response of the three UPy-contained copolymers. Figure 1 showed the dynamic strain sweep curves of the polymers at an angular frequency omega of 10 rad/s. It can be observed that PHEA-UPy presented a high storage modulus at the order of 10^7 and loss modulus with a magnitude of 10^6. When the strain is below 1%, PHEA-UPy exhibited a linear viscoelasticity with relatively constant moduli. When the strain is above 1%, PHEA-UPy presented a non-linear viscoelasticity property during the higher strain range. Furthermore, the dynamic strain sweep analysis (Figure S9a) suggests PHEA-UPy showed a typical solid state rheological property at 25 °C. For $PPEG_{360}$-UPy and $PPEG_{500}$-UPy, their moduli didn't change with the strain increasing, suggesting they both presented obvious linear viscoelasticity in the strain range from 0.1% to 100%. And the storage (G') and loss modulus (G'') of $PPEG_{360}$-UPy and $PPEG_{500}$-UPy are at magnitudes of 10^4 and 10^3, respectively, which are lower than

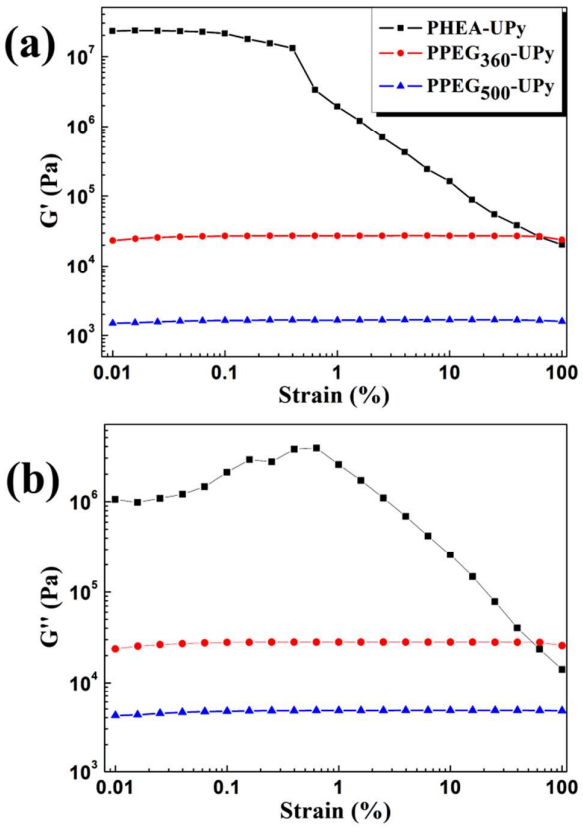

Figure 1. storage modulus (G') and loss modulus (G'') values against strain during the dynamic strain sweep.

that of PHEA-UPy due to their lower T_g. It is notable that the G'' is bigger than G' for both of $PPEG_{360}$-UPy and $PPEG_{500}$-UPy polymers. These results indicated that at 25 °C $PPEG_{360}$-UPy and $PPEG_{500}$-UPy polymers presented dominant viscous behavior, which resulted from the presence of longer flexible side chains. It is worth noting that the moduli of control polymer $PPEG_{500}$ are one magnitude lower than that of $PPEG_{500}$-UPy (see Figure S9d), indicating the UPy group enhanced the intermolecular interactions of polymer chains via hydrogen-bonding and therefore increased the moduli.

Then the dynamic mechanical investigations were carried out at linear viscoelasticity region, which is strain of 1% for PHEA-UPy and 5% for $PPEG_{360}$-UPy and $PPEG_{500}$-UPy. Figure 2 shows the dynamic frequency sweep spectra of the polymers. It can be seen that within a frequency range from 0.1 to 100 rad/s, PHEA-UPy displayed solid-like behavior and the moduli didn't change with the frequency. For $PPEG_{360}$-UPy and $PPEG_{500}$-UPy, storage and loss modulus increased with the angular frequency increasing. In high frequency region, the polymer chains of $PPEG_{360}$-UPy and $PPEG_{500}$-UPy with soft flexible side chains aren't able to eliminate the deformation in

short time via chain mobility, leading to increasing moduli. While in low frequency region, the deformation can be recovered in long time, so the polymers presented decreased moduli. In the dynamic frequency sweep spectra of $PPEG_{360}$-UPy (Figure S10b), it is found there were crossover frequencies between G' and G''. At low frequency region G' value is lower than G'' value,

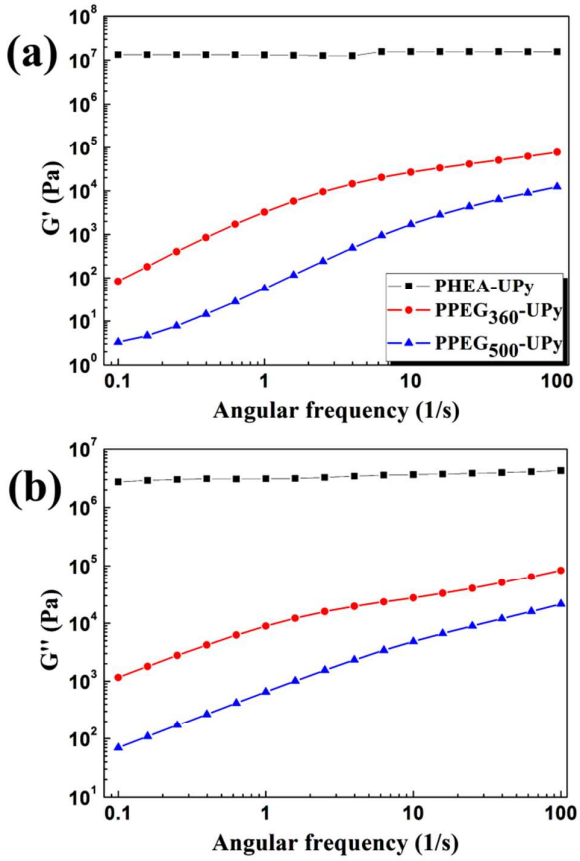

Figure 2. Dynamic frequency sweep for PHEA-UPy (angular frequency from 0.1–100 rad/s, strain kept at 1%), $PPEG_{360}$-UPy and $PPEG_{500}$-UPy (angular frequency from 0.1–100 rad/s, strain kept at 5%): storage (G') and loss modulus (G'').

while at frequency higher than crossover point G' value becomes higher than G'' value. This result indicates that $PPEG_{360}$-UPy presented dominant elastic property in high frequency. Though there is no crossover between G' and G'' for $PPEG_{500}$-UPy (Figure S10c), the G' increased more rapidly than G'' in high frequency region. As for $PPEG_{500}$, the G' is one order smaller than $PPEG_{500}$-UPy (Figure S10d) and still much lower than G'' even at high frequency. These results can be attributed to the effect of multiple H-bonding UPy group, which strengthened the interactions between polymer chains and therefore significantly enhanced the elasticity property of the UPy-based polymers at high frequency. It is worth noting that compared with $PPEG_{360}$-UPy, the strengthened interactions of UPy group for $PPEG_{500}$-UPy is less obvious, which may be resulted from that the longer side chain of $PPEG_{500}$-UPy restricted the dimerization of UPy side chains.

Self-healing study

The UPy groups are supposed to offer the polymers capability of self-healing via the reestablishment of the multiple H-bonds. To demonstrate the self-healing potential of these UPy-based copolymers at ambient environments, they were melted firstly, spread on glass substrates and then cooled down to ambient temperature to generate films. Then the films were cut by a razor blade to create cracks and placed in the ambient temperature. CCD camera was utilized to track the healing process of the cracks. Figure 3 shows the healing process of those films taken at different time after the crack production. For PHEA-UPy copolymer, as shown in Figure S11, the film didn't heal the crack even 4 hours later at ambient environment. Sun has reported a polyelectrolyte coating that can self-heal with assistant of water.[23] Because HEA is water soluble, we also tried to reveal the humility effect on the healing process of the PHEA-UPy film. After crack production, the PHEA-UPy film was placed under an environment with a relative humility of 50%. As shown in Figure 3a, it was clearly observed that the crack was completely healed within 2 h. For $PPEG_{360}$-UPy copolymer (Figure 3b), 50 minutes after the crack generation, the film spontaneously healed the crack at ambient temperature without any other treatments. As for $PPEG_{500}$-UPy (Figure 3c), the self-healing process at ambient environment was completely finished within 20 min. The repeatable self-healing abilities of these copolymers were also investigated (as shown in Figure S12), indicative of that they all presented excellent repeatable self-healing properties.

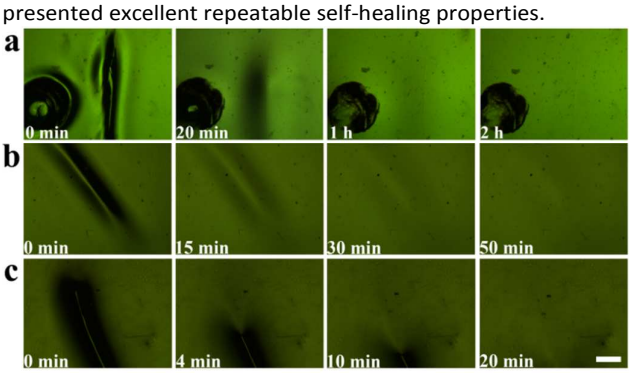

Figure 3. Self-healing processes of PHEA-UPy (a) at ambient temperature with a relative humidity of 50 %, and $PPEG_{360}$-UPy (b) and $PPEG_{500}$-UPy films (c) at ambient temperature without special humidity treatment. Scale bar: 400 μm.

The polymers presented different healing abilities. And these results can be attributed to their molecular mobility difference. PHEA-UPy has a T_g of 45 °C higher than room temperature owing to the short side chain. The rheological study revealed that PHEA-UPy exhibited solid-like property at room temperature. Therefore, the healing process of PEHA-UPy at r.t. was difficult to be achieved due to the lack of molecular mobility at temperature below T_g. While the PHEA-UPy film was placed under environment with relative humility of 50 %, the humility could soften the PHEA-UPy film surface and provide the polymer chain ability of diffusion and allowed the reestablishment of H-bonding at the interface. Compared with PHEA-UPy, $PPEG_{360}$-UPy and $PPEG_{500}$-UPy polymers have longer flexible side chains. It was recently reported that the

flexible chains allowed the functional moieties at the interface to rapidly reestablish hydrogen binding networks, which led to an increase in the healing speed.[41] The longer flexible chains ensure low T_g and sufficient chain mobility at the interface, allowing the polymer chains to diffuse and back into contact under the effect of the dimerization of UPy and then easily to form multiple H-bonding at the interface.

Adhesion and Surface interactions

Due to the high molecular polarity that originated from the hydroxyl group and the ether bond of the side chains, the prepared polymers PHEA-UPy, $PPEG_{360}$-UPy and $PPEG_{500}$-UPy may present interesting surficial or interfacial properties. Then the surface properties of the prepared polymers were investigated through the surface free energy measurements. As developed by van Oss et al.,[42] by measuring the contact angle of three probe liquids (e.g., water, diiodomethane and ethylene glycol), the surface energy (SE) can be determined according to the Young's equation showed below:

$$\gamma_L\,(\cos\theta + 1) = 2\left(\sqrt{\gamma_S^{LW}\gamma_L^{LW}} + \sqrt{\gamma_S^{+}\gamma_L^{-}} + \sqrt{\gamma_S^{-}\gamma_L^{+}}\right) \qquad (1)$$

where ϑ is the contact angle of the liquid droplet on solid surface. The equation describes the relationship of surface energy of solid phase (γ_S), surface energy of liquid phase or surface tension (γ_L) and the solid-liquid phase interfacial energy (γ_{SL}) in solid/phase/air three-phase system. Based on van Oss method, the surface energy is comprised of two contributions: Lifshitz-van der Waals (γ^{LW}) and Lewis acid-base (γ^{AB}) interactions, where γ^+ and γ^- are defined as Lewis acid and base interactions, respectively.

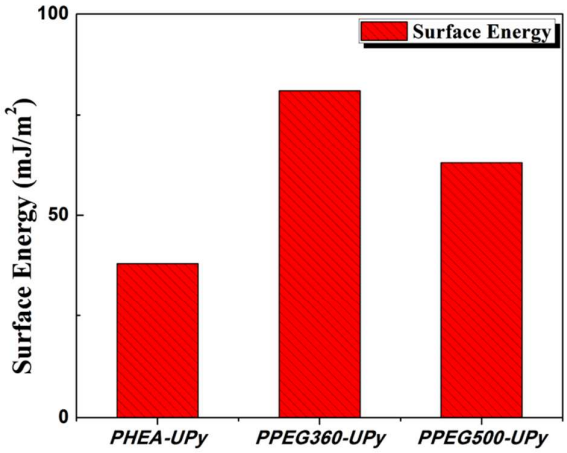

Figure 4. Surface energies (SEs) of the prepared polymers estimated from the contact angle measurements.

According to previously reported,[43] the γ^{LW} and γ^{AB} of the surface energy of polymers can be determined by measuring the contact angle using three probe liquids method and the above equations. In our work, water, diiodomethane and ethylene glycol were employed as three probe liquids. The surface free energies γ of the polymers are shown in Figure 4 on the basis of the contact angle measurements and the equations. From Figure 4, the surface energies of PHEA-UPy, $PPEG_{360}$-UPy and $PPEG_{500}$-UPy polymers were estimated to be 38, 81 and 63 mJ/m^2, respectively. PHEA-UPy has the relatively lowest surface energy. Compared with PHEA-UPy, $PPEG_{360}$-UPy and $PPEG_{500}$-UPy clearly presented enhanced surface energy. This result can be contributed to the molecular polarity effect to the surface energy. The polar and dispersion components of surface energies of the polymers were listed in Table S2. Because of the presence of PEG oligomer side chains which can be considered as polar functional group in polymer $PPEG_{360}$-UPy and $PPEG_{500}$-UPy, they both had higher molecular polarity than HEA monomer, therefore presenting drastically enhanced surface energy. It was notable that compared with the reported PBA-UPy polymers,[32] $PPEG_{360}$-UPy and $PPEG_{500}$-UPy presented higher surface energies.

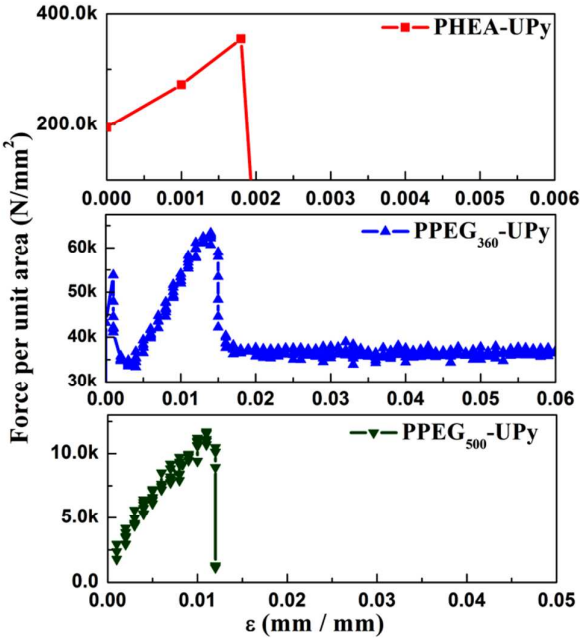

Figure 5. The 180 ° peel test results (adhesion strength) of the polymers PHEA-UPy, $PPEG_{360}$-UPy and $PPEG_{500}$-UPy revealed by tensile test mode.

Due to their high surface energy, this kind of Upy-contained copolymer may be potential in application as adhesives. Then we further investigated the adhesion strength of the three copolymers via a 180 ° peel test method. Figure 5 presents the 180 ° peel test results of the prepared copolymers at ambient temperature. It is clearly observed that PHEA-UPy, with solid-like behavior at room temperature, was detached quickly from the substrate surface, and the adhesion strength was evaluated as 355 kN/m^2. $PPEG_{360}$-UPy and $PPEG_{500}$-UPy polymers, which show dominant viscous properties at 25 °C, present relatively lower adhesion strengths of 63 and 12 kN/m^2, respectively. Based on the rheological study, PHEA-UPy presented dominant solid-like elastic property, and $PPEG_{360}$-UPy and $PPEG_{500}$-UPy showed dominant viscous property at r.t. Because PHEA-UPy exhibits higher cohesive energy based on its stronger intermolecular interactions at room temperature, the adhesion strength of PHEA-UPy is higher than that of $PPEG_{360}$-UPy and $PPEG_{500}$-UPy polymers. This also can be seen from the images of interfaces of polymers and steel substrates after the adhesion tests as shown in Figure S14. Therefore, it is

expecting PHEA-UPy being used as adhesive with self-healing ability working at room temperature. Due to their lower T_g values, $PPEG_{360}$-UPy and $PPEG_{500}$-UPy might be potential adhesives working at lower temperatures.

Conclusions

In conclusion, in this work UPy-based copolymers with self-healing ability were prepared. The effects of side chain length on polymer properties, surface properties and healing abilities were investigated, offering versatility in tuning the structures and properties. These polymers can achieve the healing of interfacial surfaces and may be potential of being applied as adhesives that used in different temperatures. This work may provide a new idea for the design of functional self-healing polymers. Furthermore, the biocompatible nature of the copolymers with PEG oligomer side chains might have potential application in biological fields such as tissue engineering.

Acknowledgements

This research was supported by 973 Projects (2012CB933803, 2014CB643605), the National Science Fund for Distinguished Young Scholars (50925310), the National Science Foundation of China (21374060, 51173103), and the Excellent Academic Leaders of Shanghai (11XD1403000). The authors also thank Dr. Kun Cui for (Shanghai Institute of Organic Chemistry, Chinese Academy of Science) for providing supports on rheological property measurements.

Notes and references

1. E. B. Murphy and F. Wudl, *Prog. Polym. Sci.*, 2010, **35**, 223-251.
2. Y. Yang and M. W. Urban, *Chem. Soc. Rev.*, 2013, **42**, 7446-7467.
3. B. J. Blaiszik, S. L. B. Kramer, S. C. Olugebefola, J. S. Moore, N. R. Sottos and S. R. White, *Annu. Rev. Mater. Res.*, 2010, **40**, 179-211.
4. S. R. White, N. R. Sottos, P. H. Geubelle, J. S. Moore, M. R. Kessler, S. R. Sriram, E. N. Brown and S. Viswanathan, *Nature*, 2001, **409**, 794-797.
5. S. H. Cho, H. M. Andersson, S. R. White, N. R. Sottos and P. V. Braun, *Adv. Mater.*, 2006, **18**, 997-1000.
6. M. M. Caruso, B. J. Blaiszik, H. Jin, S. R. Schelkopf, D. S. Stradley, N. R. Sottos, S. R. White and J. S. Moore, *ACS Appl. Mater. Interfaces*, 2010, **2**, 1195-1199.
7. Y. C. Yuan, M. Z. Rong and M. Q. Zhang, *Polymer*, 2008, **49**, 2531-2541.
8. J. D. Rule, E. N. Brown, N. R. Sottos, S. R. White and J. S. Moore, *Adv. Mater.*, 2005, **17**, 205-208.
9. B. J. Blaiszik, S. L. Kramer, M. E. Grady, D. A. McIlroy, J. S. Moore, N. R. Sottos and S. R. White, *Adv. Mater.*, 2012, **24**, 398-401.
10. K. S. Toohey, N. R. Sottos, J. A. Lewis, J. S. Moore and S. R. White, *Nat. Mater.*, 2007, **6**, 581-585.
11. K. S. Toohey, C. J. Hansen, J. A. Lewis, S. R. White and N. R. Sottos, *Adv. Funct. Mater.*, 2009, **19**, 1399-1405.
12. M. Nakahata, Y. Takashima, H. Yamaguchi and A. Harada, *Nat. Commun.*, 2011, **2**, 511-516.
13. F. Herbst, S. Seiffert and W. H. Binder, *Polym. Chem.*, 2012, **3**, 3084-3092.
14. S. Bode, L. Zedler, F. H. Schacher, B. Dietzek, M. Schmitt, J. Popp, M. D. Hager and U. S. Schubert, *Adv. Mater.*, 2013, **25**, 1634-1638.
15. P. Cordier, F. Tournilhac, C. Soulie-Ziakovic and L. Leibler, *Nature*, 2008, **451**, 977-980.
16. R. Zhang, T. Yan, B.-D. Lechner, K. Schröter, Y. Liang, B. Li, F. Furtado, P. Sun and K. Saalwächter, *Macromolecules*, 2013, **46**, 1841-1850.
17. C. Wang, N. Liu, R. Allen, J. B. Tok, Y. Wu, F. Zhang, Y. Chen and Z. Bao, *Adv. Mater.*, 2013, **25**, 5785-5790.
18. K. Imato, M. Nishihara, T. Kanehara, Y. Amamoto, A. Takahara and H. Otsuka, *Angew. Chem. Int. Ed.*, 2012, **51**, 1138-1142.
19. Y. Amamoto, J. Kamada, H. Otsuka, A. Takahara and K. Matyjaszewski, *Angew. Chem. Int. Ed.* , 2011, **50**, 1660-1663.
20. X. Chen, M. A. Dam, K. Ono, A. Mal, H. Shen, S. R. Nutt, K. Sheran and F. Wudl, *Science*, 2002, **295**, 1698-1702.
21. C. Yuan, M. Z. Rong, M. Q. Zhang, Z. P. Zhang and Y. C. Yuan, *Chem. Mater.*, 2011, **23**, 5076-5081.
22. M. Burnworth, L. Tang, J. R. Kumpfer, A. J. Duncan, F. L. Beyer, G. L. Fiore, S. J. Rowan and C. Weder, *Nature*, 2011, **472**, 334-337.
23. X. Wang, F. Liu, X. Zheng and J. Sun, *Angew. Chem. Int. Ed.*, 2011, **50**, 11378-11381.
24. S. Basak, J. Nanda and A. Banerjee, *Chem. Commun.*, 2014, **50**, 2356-2359.
25. M. Krogsgaard, M. A. Behrens, J. S. Pedersen and H. Birkedal, *Biomacromolecules*, 2013, **14**, 297-301.
26. A. Vidyasagar, K. Handore and K. M. Sureshan, *Angew. Chem .Int. Ed.*, 2011, **50**, 8021-8024.
27. B. C. Tee, C. Wang, R. Allen and Z. Bao, *Nat. Nanotechnol.*, 2012, **7**, 825-832.
28. J. Liu, G. Song, C. He and H. Wang, *Macromol. Rapid Commun.*, 2013, **34**, 1002-1007.
29. Y. Chen, A. M. Kushner, G. A. Williams and Z. Guan, *Nat. Chem.*, 2012, **4**, 467-472.
30. F. H. Beijer, R. P. Sijbesma, H. Kooijman, A. L. Spek and E. W. Meijer, *J. Am. Chem. Soc.*, 1998, **120**, 6761-6769.
31. J. Cui and A. del Campo, *Chem. Commun.*, 2012, **48**, 9302-9304.
32. A. Faghihnejad, K. E. Feldman, J. Yu, M. V. Tirrell, J. N. Israelachvili, C. J. Hawker, E. J. Kramer and H. Zeng, *Adv. Funct. Mater.*, 2014, **24**, 2322-2333.
33. P. Y. Lee, E. Cobain, J. Huard and L. Huang, *Mol. Ther.*, 2007, **15**, 1189-1194.
34. Y. Zhang, B. Yang, X. Zhang, L. Xu, L. Tao, S. Li and Y. Wei, *Chem. Commun.*, 2012, **48**, 9305-9307.
35. J. A. Hunt, R. Chen, T. van Veen and N. Bryan, *J. Mater. Chem B*, 2014, **2**, 5319-5338.
36. C. H. Lin, Y. H. Yeh, W. C. Lin and M. C. Yang, *Colloids and surfaces. B, Biointerfaces*, 2014, **123**, 986-994.
37. F. Bella, A. Sacco, G. P. Salvador, S. Bianco, E. Tresso, C. F. Pirri and R. Bongiovanni, *The Journal of Physical Chemistry C*, 2013, **117**, 20421-20430.
38. K. Yamauchi, J. R. Lizotte and T. E. Long, *Macromolecules*, 2003, **36**, 1083-1088.
39. W. M. Gramlich, G. Theryo and M. A. Hillmyer, *Polym. Chem.*, 2012, **3**, 1510-1516.
40. A. Muhlebach, S. G. Gaynor and K. Matyjaszewski, *Macromolecules*, 1998, **31**, 6046-6052.
41. A. Phadke, C. Zhang, B. Arman, C. C. Hsu, R. A. Mashelkar, A. K. Lele, M. J. Tauber, G. Arya and S. Varghese, *Proc. Nat. Acad. Sci. USA*, 2012, **109**, 4383-4388.
42. C. J. van Oss, M. K. Chaudhury and R. J. Good, *Adv. Colloid Interface Sci.*, 1987, **28**, 35-64.
43. F. C. Teng, H. B. Zeng and Q. X. Liu, *J. Phys. Chem. C*, 2011, **115**, 17485-17494.